HHS Public Access

Author manuscript

Sci China Life Sci. Author manuscript; available in PMC 2016 November 25.

Published in final edited form as:

Sci China Life Sci. 2016 August ; 59(8): 792–801. doi:10.1007/s11427-016-5088-4.

Binding of transition metals to S100 proteins

Benjamin A. Gilston[1], **Eric P. Skaar**[2], and **Walter J. Chazin**[1,*]

[1]Departments of Biochemistry and Chemistry, and Center for Structural Biology, Vanderbilt University, Nashville TN 37232-9717, USA

[2]Department of Pathology, Microbiology and Immunology, Vanderbilt University Medical Center, Nashville TN 37232-2561, USA

Abstract

The S100 proteins are a unique class of EF-hand Ca^{2+} binding proteins distributed in a cell-specific, tissue-specific, and cell cycle-specific manner in humans and other vertebrates. These proteins are distinguished by their distinctive homodimeric structure, both intracellular and extracellular functions, and the ability to bind transition metals at the dimer interface. Here we summarize current knowledge of S100 protein binding of Zn^{2+}, Cu^{2+} and Mn^{2+} ions, focusing on binding affinities, conformational changes that arise from metal binding, and the roles of transition metal binding in S100 protein function.

Keywords

S100 Proteins; Zinc; Manganese; Copper

INTRODUCTION

S100 proteins are an important class of EF-hand calcium binding proteins distinguished by unique dimeric structures and functions both inside and outside cells (Donato, 2003; Donato et al., 2013; Nelson and Chazin, 1998; Potts et al., 1995; Zackular et al., 2015). Their intracellular functions are primarily regulatory in nature, mediated by interactions with target proteins involved in a range of processes including proliferation, differentiation, and inflammation. S100 proteins are also released or secreted from cells, where they activate a variety of cell surface receptors in both an autocrine and a paracrine manner. Several S100 proteins serve as damage-associated molecular pattern recognition factors (DAMPS) in the adaptive and innate immune systems (Donato et al., 2013), and are known to be recruited to sites of inflammation (Striz and Trebichavsky, 2004). The S100A8/S100A9 heterodimer (termed calprotectin or CP) is the most-well studied of the S100 proteins in the immune response; it has been shown to function in the response to a range of microbial pathogens via a mechanism termed “nutritional immunity”, inhibiting growth by sequestering nutrient

*Corresponding author (walter.chazin@vanderbilt.edu).

Compliance and ethics The author(s) declare that they have no conflict of interest.

transition metals Zn^{2+} and Mn^{2+} (Zackular et al., 2015). The binding of transition metals by S100 proteins was first characterized over 30 years ago (Baudier et al., 1982, 1984). With a specific functional role for transition metal binding by S100 proteins now emerging, it is an appropriate time to review the field. In this monograph, we will focus on the wide range of affinities for these ions, the structural consequences of transition metal binding, and how transition metal binding modulates function.

S100 proteins were first identified over five decades ago from bovine brain and are named on the basis of their solubility in 100% ammonium sulfate (Moore, 1965). To date, there are 25 members in the human proteome and homo-logues have only been identified only in vertebrates, suggesting that they are “evolutionary newcomers” (Schaub and Heizmann, 2008). Unlike other EF-hand proteins, they exhibit cell-type, tissue-specific, and cell cycle-dependent expression along with differential gene regulation (Schäfer and Heizmann, 1996). S100 proteins are involved in a wide range of cellular functions including intracellular calcium buffering, modulation of enzyme activities, energy metabolism, and regulation of cell growth, cytoskeleton development and differentiation (Schaub and Heizmann, 2008). While EF-hand proteins appear to have evolved to transduce intracellular Ca^{2+} signals, S100 proteins have the unique ability to also function in the extracellular milieu. Some S100 proteins play essential roles in signaling and secretion of ligands for receptor binding (Donato et al., 2013), modulated in certain cases by post-translational modifications and transition metal binding (Moroz et al., 2009a; van Dieck et al., 2009). S100 proteins are also part of the innate immune response to bacterial pathogens (Zackular et al., 2015). In the clinic S100 proteins serve as biomarkers for cardiomyopathy (S100A1), psoriasis (S100A7), chronic inflammation disorders and inflammatory bowel disease (S100A8/A9), and several cancers (S100A2/A4/A6) (Heizmann et al., 2002; Schäfer and Heizmann, 1996).

S100 PROTEIN STRUCTURE AND BIOCHEMISTRY

The fundamental organization for all EF-hand Ca^{2+} binding proteins is a four-helix bundle domain containing a pair of helix-loop-helix EF-hand motifs (Figure 1). S100 proteins, the largest subgroup within the EF-hand superfamily, are comprised of an S100-specific N-terminal EF-hand with a 14-residue Ca^{2+} binding loop, and a C-terminal EF-hand with a canonical 12-residue Ca^{2+} binding loop (Bunick et al., 2004). They are also distinguished from other EF-hand proteins (e.g. calmodulin) by obligate formation of dimers (Figure 1) (Potts et al., 1996); all function as dimers or higher order oligomers except for calbindin D_{9k} (S100G), which is a shortened, ancestral member of the sub-family that lacks the ability to dimerize. Higher order oligomerization of S100 proteins is non-covalent and can be promoted by low affinity metal binding sites at the exterior surface of the dimer. Both Ca^{2+} and transition metals (particularly Zn^{2+}) have been shown to stimulate oligomerization *in vitro*, and crystal structures have revealed a range of oligomeric states. However, the relevance of oligomerization of S100 proteins *in vivo* remains controversial except in situations where protein and metal concentrations are sufficiently high to match the conditions of the *in vitro* experiments. That stated, the high (millimolar) concentration of Ca^{2+} in the extracellular space implies that those S100 proteins whose oligomerization is promoted by Ca^{2+} may exist in higher order oligomeric states.

Like other EF-hand proteins, S100 proteins respond to Ca^{2+} signals by undergoing conformational changes upon ion binding, although the conformational changes are more modest relative to canonical EF-hand Ca^{2+} sensor proteins such as calmodulin (Nelson and Chazin, 1998; Nelson et al., 2002). Despite large variations in amino acid sequence (between 20% and 60% identity), the Ca^{2+}-induced conformational change in all S100 proteins involves a significant shift in the orientation of Helix III (Figure 2) (Maler et al., 2002). Like other EF-hand Ca^{2+} sensors, this conformational change results in exposure of a hydrophobic patch that serves as the key factor driving binding of targets. Although they have very similar structural architectures, S100 proteins interact with a diverse set of cellular targets. This variability is accomplished by the fine-tuning within the target binding site of each S100 protein (Bhattacharya et al., 2004), in combination with their distinct cell-type, tissue-specific, and cell cycle-dependent expression. Current understanding of the cooperativity of Ca^{2+} binding and the structural rearrangements induced by Ca^{2+} binding have been reviewed in more detail elsewhere (Chazin, 2007; Ikura, 1996; Nelson and Chazin, 1998). Here we will focus on the unique ability of S100 proteins to bind transition metals in binding sites distinct from their Ca^{2+} binding sites (Heizmann and Cox, 1998), and the corresponding effects on structure, function and biochemical properties.

BINDING OF ZINC

The first report of Zn^{2+} binding to an S100 protein (S100B) was over thirty years ago (Baudier et al., 1984). Since that time binding of Zn^{2+} has been reported for S100A1, S100A2, S100A3, S100A5, S100A6, S100A7, S100A8/A9, S100A12, S100A16 and S100B (Table 1). Zn^{2+} binding S100 proteins can be classified into two categories: His-rich and Cys-rich. Sequence alignments, spectroscopic analysis, site-directed mutagenesis and high-resolution structures revealed a conserved binding motif for the proteins with His-rich sites (S100A6, S100A7, S100A8/A9, S100A12, S100A15, S100B), with 4 His residues, or 3 His and 1 Asp residues, at the dimer interface (Figure 3). The first Zn^{2+}-bound structure was determined for S100A7 (Brodersen et al., 1999), and several additional Zn^{2+}-bound structures from the His-rich group have been reported since. Since the proteins are dimers, each protein binds two Zn^{2+} at the two symmetrically disposed sites (Figure 2).

The S100 proteins capable of binding Zn^{2+} ions have affinities ranging from K_d=4 nmol L^{-1} (S100A3) to 100 μmol L^{-1} (S100A7) (Table 1). Direct comparisons among the reported affinities are not straightforward because the methods used and experimental conditions vary significantly. Importantly, although the majority of the K_d values fall within the μmol L^{-1} range, Zn^{2+} concentrations inside and outside cells are low (e.g. 2–10 nmol L^{-1} in the cytoplasm). Hence, the biological relevance of the binding of Zn^{2+} has yet to be established for most S100 proteins. Another significant factor in correlating *in vitro* measurements to functional context is the energetic coupling of interactions with metal co-factors and targets. This issue is well recognized for EF-hand proteins in the case of the substantial differences in Ca^{2+} affinity measured in the absence and presence of target proteins. Thus, an interplay between Zn^{2+} and Ca^{2+} binding to S100 proteins is expected. In fact, Zn^{2+} binding has been reported to raise the Ca^{2+} affinity of S100B by a factor of 10 and of S10012 by ~1500 fold (Dell'Angelica et al., 1994; Moroz et al., 2011), to lower the Ca^{2+} affinity of S100A2 (Koch et al., 2007), and to have no effect on S100A5 (Schäfer et al., 2000).

The effects of Zn^{2+} binding on the structure of S100 proteins are in general rather modest. The basic dimeric architecture observed for the apo and Ca^{2+}-loaded states is retained and overall the structures are very similar (all Cα RMSDs (root-mean-square deviations)<1.0 Å) (Figure 2A). The structural changes induced by the binding of Ca^{2+} are substantially larger than the structural changes induced by the binding of Zn^{2+}, i.e. Zn^{2+}-bound apo proteins are more similar to the apo state than to the Zn^{2+}-bound Ca^{2+}-loaded state, and Zn^{2+}-bound Ca^{2+}-loaded proteins are more similar to the Ca^{2+}-loaded state than to the Zn^{2+}-bound apo state (Figure 2B). Detailed comparative analyses for structural differences between all states are possible for S100A7, for which structures have been determined in the apo, Ca^{2+}-loaded, and Ca^{2+}, Zn^{2+}-loaded states, and for S100A12, for which structures have been determined in the apo, Ca^{2+}-loaded, Zn^{2+}-loaded, and Ca^{2+},Cu^{2+}-loaded states. (The great similarity of Zn^{2+} and Cu^{2+} sites is discussed below in “Binding of copper”) As seen in the Zn^{2+}-loaded structures of S100A7 and S100A12, two Zn^{2+} ions are bound at the symmetrically disposed sites (Figure 4), coordinated by three His N2 atoms (His17, His86, His90) and an aspartate side chain (Asp24) (Figure 4B) (Brodersen et al., 1999; Leon et al., 2009). In all cases, the primary effect of Zn^{2+} is to alter the orientation of Helix III (Figure 2B). Interestingly, Zn^{2+}-binding results in poor electron density for residues 62–67 in S100A12, even though these are well defined in the structure of the apo state (Moroz et al., 2009a). This led to the proposal that flexibility in this loop region may be induced by Zn^{2+}, and thereby facilitate the ~1500-fold increase in the affinity of S100A12 for Ca^{2+}.

The binding of Zn^{2+} has been extensively studied for S100B, most notably in conjunction with the p53 tumor suppressor protein (Lin et al., 2004). S100B has high affinity for Zn^{2+} (K_d ~90 nmol L^{-1}). NMR spectroscopy and site directed mutagenesis indicated that Zn^{2+} binding occurs in a similar manner to other S100 proteins with His-rich transition metal binding sites, namely His15/His25 from one subunit and His85/His89 from the other subunit. However, Zn^{2+} binding to S100B causes a more pronounced kink in Helix IV than in S100A7 and S100A12 (Wilder et al., 2005). Zn^{2+} binding has been shown to increase the affinity for target peptides over the effect of Ca^{2+} alone (Wilder et al., 2003). Structural coupling of the Zn^{2+} and target binding sites has been found, and this information has been incorporated into the design of S100B inhibitors of the interaction with targets such as p53. Co-crystal structures with pentamidine, an S100B inhibitor known to bind in the target binding site, were determined for both the Ca^{2+}- and Ca^{2+}, Zn^{2+}-loaded states (Charpentier et al., 2008; Charpentier et al., 2009). These studies motivated the generation of new inhibitors engineered to disrupt the Zn^{2+}-binding residues and Zn^{2+}-induced conformational changes in S100B (Cavalier et al., 2014).

The role of oligomerization in the function of S100 proteins has been vigorously debated. There is ample evidence of Ca^{2+}- and Zn^{2+}-induced oligomerization *in vitro* including a number of crystal structures with high order oligomerization states (Moroz et al., 2002, 2009a; Ostendorp et al., 2007) and a mass spectrometry study of Zn^{2+}-induced tetramerization of CP (Vogl et al., 2006). However, there is very little evidence of the functional significance of oligomerization from experiments in cells; this is an area that is in great need of further investigation. A role for oligomerization of S100 proteins is most likely in association with the extracellular functions of S100 proteins as activators of cell surface receptors (Malashkevich et al., 2010; Moroz et al., 2009a; Ostendorp et al., 2011, 2007). The

most well studied of these receptors is receptor for advanced glycation end products (RAGE), which has been shown to bind several S100 proteins at the cell surface and elicit an intracellular response via the NF-κB signaling pathway. A role for Zn^{2+} in the interaction of S100A7 and S100A15 with RAGE has been proposed (Murray et al., 2012; Wolf et al., 2008).

The Cys-rich Zn^{2+} binding S100 proteins (S100A2, S100A3, S100A4) are much less studied than the His-rich group (Moroz et al., 2011). One challenge is the absence of a conserved motif evident from alignment of these proteins (Figure 3). The consensus view is that the Cys-rich sites coordinate Zn^{2+} ions with either 4 Cys residues or 3 Cys and 1 His residue (Moroz et al., 2011). A second challenge is that Cys-rich sites will be susceptible to redox reactions that disrupt disulfides and modulate Zn^{2+}-binding. Obtaining high resolution X-ray data on the Cys-rich Zn^{2+}-binding S100 proteins is difficult due to improper folding during *in vitro* bacterial overexpression. In fact, the majority of S100A2 and S100A4 structures were determined with Cys residues mutated to facilitate protein production. The protein production obstacle was overcome for S100A3 by producing the protein from insect cells, which promotes proper disulfide formation and folding (Kizawa et al., 2013a, b). Crystallization of S100A3 produced in this manner identified two disulfide bonds not previously identified. These disulfides apparently play a critical structural role, as disruption of either disulfide significantly affected the Ca^{2+} affinity (Unno et al., 2011). Unfortunately, electron density for Zn^{2+} ions was too weak to formally assign their presence in the structure. However, a single Cys-rich Zn^{2+} site could be readily modeled, and Zn^{2+} binding was proposed to be important for folding and formation of the critical disulfide bonds in S100A3. Since the majority of analyses in the past 15 years utilized recombinant protein expressed in *E. coli*, future studies using proteins produced from eukaryotic expression systems may enhance understanding of Zn^{2+} binding to S100 proteins from the Cys-rich group.

BINDING OF COPPER

Due to their similar chemical properties, copper is anticipated to bind to most zinc binding sites in proteins. It was therefore natural to examine the binding of copper (Cu^{2+}) to S100 proteins when Zn^{2+} binding was first noted for S100B (Nishikawa et al., 1997). In that report, four Cu^{2+} ions were identified per S100B dimer with an average dissociation constant (K_d) of 0.46 μmol L^{-1}. However, subsequent structure-based alignments predicted that there are only two high affinity sites and that the two others are weak non-specific sites (Nishikawa et al., 1997). Ion competition experiments demonstrated that the Cu^{2+} ions could be displaced by Zn^{2+}, but not Ca^{2+}. Thus, as expected, the binding of Cu^{2+} by S100 proteins closely resembles binding of Zn^{2+}, with a few noticeable exceptions.

Important insight into binding of Cu^{2+} by S100 proteins was provided by the X-ray crystal structure of Ca^{2+}, Cu^{2+}-S100A12 (Moroz et al., 2003). The overall conformational change induced by the binding of Cu^{2+} is very small; the Cα RMSD of the Ca^{2+} versus the Ca^{2+}, Cu^{2+} state is 0.35 Å. Interestingly, both the apo and Ca^{2+}, Cu^{2+}-bound states have well defined electron density out to Lys90, but His87-Lys90 is disordered when only Ca^{2+} is bound (Moroz et al., 2003). The Cu^{2+} ion is bound in a canonical Cu^{2+} site (3 His residues

along with either an oxygen or sulfur containing residue), with coordination by His15 and Asp25 from one subunit and His85 and His89 from the other subunit, identical to the coordination of Zn^{2+}. In fact, Ca^{2+}, Cu^{2+} and Ca^{2+}, Zn^{2+} structures are very similar even when comparing between different S100 proteins (Figure 4): the Cα RMSD between Ca^{2+}, Cu^{2+}-S100A12 and Ca^{2+}, Zn^{2+}-S100A7 is only 0.72 Å, and for Ca^{2+}, Zn^{2+}-S100B only 0.42 Å (Charpentier et al., 2008). The great similarity in the structures of the Cu^{2+} and Zn^{2+}-loaded protein implies that Cu^{2+} will bind to the Zn^{2+} sites in other S100 proteins (Moroz et al., 2003, 2009b).

The structural consequences of Cu^{2+} binding to S100A13 have been investigated using solution NMR (Arnesano et al., 2005). Comparisons between apo, Ca^{2+}-loaded and Ca^{2+}, Cu^{2+}-loaded S100A13 revealed Cu^{2+} causes an additional, minor opening of the Helix III-IV interface relative to the Ca^{2+}-loaded state. The binding site has several unique characteristics compared to other S100 proteins, including the location of the site, as well as the ligand coordination and solvent accessibility to the Cu^{2+} ion. NMR titrations of Ca^{2+}-S100A13 with paramagnetic Cu^{2+} ions were used to propose Glu4, Glu8, Glu11, and His48 as the Cu^{2+}-chelating side chains. These correlated with electron paramagnetic resonance (EPR) studies that assigned the Cu^{2+} coordination as pseudo-tetragonal with nitrogen and oxygen donor atoms. An unexpected aspect of their analysis was that the Cu^{2+} ions are completely exposed to solvent, unlike the typical transition metal sites that are buried within the S100 proteins (Arnesano et al., 2005). The authors suggested that exposure of the metal may help regulate the interaction of S100A13 with target proteins, but no data was provided in support of this speculation.

Zn^{2+} and Cu^{2+} ions have been proposed to induce conformational changes in S100 proteins (e.g. (Vogl et al., 2006)), although the crystal structures described above and shown in Figure 4 reveal these changes are very modest. Nevertheless, Cu^{2+} binding has the potential to alter the structure of S100 proteins and therefore oligomerization and interactions with target proteins. Although Zn^{2+} induced oligomerization of S100 proteins has been explored *in vitro*, the sole study of the effect of Cu^{2+} reported no changes in oligomerization of the S100A8/S100A9 heterodimer (Vogl et al., 2006). The only study of the effect of Cu^{2+} on receptor binding revealed stimulation of the interaction of S100A4 with RAGE (Haase-Kohn et al., 2011). Although the dearth of information about the effects of Cu^{2+} on physical properties should be addressed, there is even greater urgency to establish if Cu^{2+} binding has any physiological role in S100 protein function.

BINDING OF MANGANESE

Manganese is an important transition metal in biological systems (Sigel and Sigel, 2000). It is a critical component in certain enzymatic processes (e.g. phosphorylation) and in the oxidative stress response. Recently, manganese regulation has been recognized for its essential role in contributing to the virulence of pathogenic organisms (reviewed in (Zackular et al., 2015)), with an explicit role played by the S100A8/S100A9 heterodimer, calprotectin (CP). As will be summarized below, high affinity binding of Mn^{2+} to S100 proteins is unique to CP.

All pathogenic organisms require essential nutrients from the host to survive and proliferate, including transition metals. A mechanism termed nutritional immunity, which involves sequestering the essential nutrients from the pathogen, is used by the host to fight infection. A role for transition metals besides Fe in nutritional immunity was first discovered when inductively coupled plasma mass spec-trometry (ICP-MS) analysis showed that there are distinct differences in the transition metal content in and around tissues infected with *Staphylococcus aureus* (Corbin et al., 2008). In particular, staphylococcal abscesses were found to be devoid of Zn^{2+} and Mn^{2+} ions. Proteomic imaging of the tissue revealed high concentrations of the S100A8 and S100A9 CP subunits surrounding the sites of infection. Subsequent work confirmed that CP, which is present in very large abundance in certain innate immune cells such as neutrophils, plays a critical role in the innate immune response to pathogens, functioning via the nutritional immunity mechanism through the high affinity binding and sequestration of Zn^{2+} and Mn^{2+} (Corbin et al., 2008; Zackular et al., 2015). Subsequent studies using CP knockout mice have demonstrated that CP inhibits growth from other pathogenic organisms, including *Acinetobacter baumannii*, *Candida albicans*, *Aspergillus fumigatus* and *Helicobacter pylori* (Clark et al., 2016; Gaddy et al., 2014; Hood et al., 2012; Kehl-Fie et al., 2011, 2013).

Based on the available information on the binding of Zn^{2+} to S100 proteins, it was assumed that Mn^{2+} bound to similar sites and completed its coordination shell with waters. Importantly, early studies showed that CP bound 2 equivalents of Zn^{2+} ions, but only one equivalent of Mn^{2+}. This was confirmed by site-directed mutagenesis studies that revealed Mn^{2+} binds to the 4-His site (His17 and His27 from S100A8, His91 and His95 from S100A9) (Kehl-Fie et al., 2011). Site directed mutagenesis experiments also showed that two His residues in the S100A9 C-terminal tail (His103, His105) are required for high affinity Mn^{2+} binding (Brophy et al., 2013; Damo et al., 2013). As noted above, there is energetic coupling of transition metal binding and Ca^{2+} binding; the Mn^{2+} affinity of CP under limited Ca^{2+} availability (K_d>550 nmol L^{-1}) is weaker than in the presence of Ca^{2+} (K_d=194 nmol L^{-1}) (Brophy and Nolan, 2015; Damo et al., 2013). The origin of this allosteric effect has yet to be established, although it is conceivable that binding of Ca^{2+} results in reorganization of the structure and/or dynamics of key side chains to better facilitate Mn^{2+} binding. Notably, the only known function of transition metal binding for CP is in the extracellular milieu where Ca^{2+} concentrations are very high (in the mmol L^{-1} range) and CP's Ca^{2+} sites will invariably be filled, so the physiological relevance of the difference in Mn^{2+} affinities in the absence and presence of Ca^{2+} remains uncertain.

The critical step forward in characterizing the binding of Mn^{2+} to CP was the determination of the crystal structure of $(Ca^{2+})_4$, Mn^{2+}-CP (Brophy et al., 2013; Damo et al., 2013; Gagnon et al., 2015) (Figure 5). Comparison with the $(Ca^{2+})_4$-CP structure (Korndorfer et al., 2007) revealed there are no large conformational changes. The Cα RMSD between the two structures is 0.29 Å for the S100A8 subunit and 0.24 Å for the S100A9 subunit. Previous crystal structures of CP were disordered beyond His95 in the C-terminal tail; only with the addition of Mn^{2+} ions in the crystal structure was electron density out to Gly112 well defined. This correlates with the direct observation of chelation of the Mn^{2+} ion by the His103 and His105 side chains. Typically, Mn^{2+} is coordinated by 5 or 6 ligands. The Mn^{2+} site in CP is the only example of 6-His octahedral coordination of Mn^{2+} in the Protein

DataBank (PDB). CP is the only member of the S100 protein group that is capable of high affinity binding of Mn^{2+} (Brophy et al., 2013; Brophy and Nolan, 2015; Damo et al., 2013); the crystal structure shows that this is due to the unique combination of the 4-His transition metal binding site at the heterodimer interface (Figure 5) and the His-rich C-terminal tail that is unique to S100A9.

BINDING OF OTHER TRANSITION METALS

Robust Zn^{2+} binding at the dimerization interface led to studies of the ability of S100 proteins to bind other first-row transition metals besides Mn^{2+} and Cu^{2+}, but no significant affinities were observed (Fritz et al., 1998). A recent study reports that CP is capable of sequestering ferrous (Fe^{2+}) iron from pathogenic growth media, in parallel to sequestration of Mn^{2+} and Zn^{2+} (Nakashige et al., 2015). However, the relevance of ferrous iron to the host-pathogen interaction has not been firmly established, and existing *in vivo* data do not support a role for CP in the sequestration of iron as a defense strategy against infection (Corbin et al., 2008; Damo et al., 2013). Sub-picomolar affinity for Fe^{2+} was reported, with coordination via an uncommon 6-His coordination assigned based on Mössbauer spectroscopy (Nakashige et al., 2015) that presumably corresponds to the unique Mn^{2+} binding site in CP. If such very high CP affinity for Fe^{2+} CP is validated, a role for CP-dependent Fe^{2+} sequestration during infection will need to be investigated.

CONCLUDING REMARKS

The ability of S100 proteins to bind transition metals at sites separate from their Ca^{2+} binding sites highlights the complexities of their biochemical actions and the everchanging environments within and outside cells. Structural analyses have identified specific conformational changes induced by Ca^{2+} and transition metals. However, information is urgently needed to understand if and how transition metals modulate S100 protein interactions with their targets. Questions regarding oligomerization state and whether transition metal binding is needed for signaling to occur also need to be addressed. Substantial evidence for S100 proteins in human disease suggests there is significant potential in pursuing S100 proteins as therapeutic targets and motivates ongoing efforts in multiple laboratories to develop S100 protein-specific inhibitors.

Acknowledgements

This work was supported by operating grant (R01 AI101171 to Eric P. Skaar and Walter J. Chazin), and institutional training grant (T32 ES007028 support for Benjamin A. Gilston) from the US National Institutes of Health.

References

Arnesano F, Banci L, Bertini I, Fantoni A, Tenori L, Viezzoli MS. Structural interplay between calcium(II) and copper(II) binding to S100A13 protein. Angew Chem Int Ed Engl. 2005; 44:6341–6344. [PubMed: 16145699]

Baudier J, Glasser N, Gerard D. Ions binding to s100 proteins. I. Calcium- and zinc-binding properties of bovine brain s100 alpha alpha, s100a (alpha beta), and s100b (beta beta) protein: Zn^{2+} regulates Ca^{2+} binding on s100b protein. J Biol Chem. 1986; 261:8192–8203. [PubMed: 3722149]

Baudier J, Glasser N, Haglid K, Gerard D. Purification, characterization and ion binding properties of human brain S100b protein. Biochim Biophys Acta. 1984; 790:164–173. [PubMed: 6487634]

Baudier J, Holtzscherer C, Gerard D. Zinc-dependent affinity chromatography of the S100b protein on phenyl-Sepharose. A rapid purification method. FEBS Lett. 1982; 148:231–234. [PubMed: 7152019]

Bhattacharya S, Bunick CG, Chazin WJ. Target selectivity in EF-hand calcium binding proteins. Biochim Biophys Acta. 2004; 1742:69–79. [PubMed: 15590057]

Brodersen DE, Nyborg J, Kjeldgaard M. Zinc-binding site of an S100 protein revealed. Two crystal structures of Ca^{2+}-bound human psoriasin (S100A7) in the Zn^{2+}-loaded and Zn^{2+}-free states. Biochemistry. 1999; 38:1695–1704. [PubMed: 10026247]

Brophy MB, Nolan EM. Manganese and microbial pathogenesis: sequestration by the Mammalian immune system and utilization by microorganisms. ACS Chem Biol. 2015; 10:641–651. [PubMed: 25594606]

Brophy MB, Hayden JA, Nolan EM. Calcium ion gradients modulate the zinc affinity and antibacterial activity of human calprotectin. J Am Chem Soc. 2012; 134:18089–18100. [PubMed: 23082970]

Brophy MB, Nakashige TG, Gaillard A, Nolan EM. Contributions of the S100A9 C-terminal tail to high-affinity Mn(II) chelation by the host-defense protein human calprotectin. J Am Chem Soc. 2013; 135:17804–17817. [PubMed: 24245608]

Bunick CG, Nelson MR, Mangahas S, Hunter MJ, Sheehan JH, Mizoue LS, Bunick GJ, Chazin WJ. Designing sequence to control protein function in an EF-hand protein. J Am Chem Soc. 2004; 126:5990–5998. [PubMed: 15137763]

Cavalier MC, Pierce AD, Wilder PT, Alasady MJ, Hartman KG, Neau DB, Foley TL, Jadhav A, Maloney DJ, Simeonov A, Toth EA, Weber DJ. Covalent small molecule inhibitors of Ca^{2+}-bound S100B. Biochemistry. 2014; 53:6628–6640. [PubMed: 25268459]

Charpentier TH, Wilder PT, Liriano MA, Varney KM, Pozharski E, MacKerell AD Jr. Coop A, Toth EA, Weber DJ. Divalent metal ion complexes of S100B in the absence and presence of pentamidine. J Mol Biol. 2008; 382:56–73. [PubMed: 18602402]

Charpentier TH, Wilder PT, Liriano MA, Varney KM, Zhong S, Coop A, Pozharski E, MacKerell AD Jr. Toth EA, Weber DJ. Small molecules bound to unique sites in the target protein binding cleft of calcium-bound S100B as characterized by nuclear magnetic resonance and X-ray crystallography. Biochemistry. 2009; 48:6202–6212. [PubMed: 19469484]

Chazin WJ. The impact of X-ray crystallography and NMR on intracellular calcium signal transduction by EF-hand proteins: crossing the threshold from structure to biology and medicine. Sci STKE. 2007; 2007:pe27. [PubMed: 17536097]

Clark HL, Jhingran A, Sun Y, Vareechon C, de Jesus Carrion S, Skaar EP, Chazin WJ, Calera JA, Hohl TM, Pearlman E. Zinc and manganese chelation by neutrophil S100A8/A9 (Calprotectin) limits extracellular *Aspergillus fumigatus* hyphal growth and corneal infection. J Immunol. 2016; 196:336–344. [PubMed: 26582948]

Corbin BD, Seeley EH, Raab A, Feldmann J, Miller MR, Torres VJ, Anderson KL, Dattilo BM, Dunman PM, Gerads R, Caprioli RM, Nacken W, Chazin WJ, Skaar EP. Metal chelation and inhibition of bacterial growth in tissue abscesses. Science. 2008; 319:962–965. [PubMed: 18276893]

Damo SM, Kehl-Fie TE, Sugitani N, Holt ME, Rathi S, Murphy WJ, Zhang Y, Betz C, Hench L, Fritz G, Skaar EP, Chazin WJ. Molecular basis for manganese sequestration by calprotectin and roles in the innate immune response to invading bacterial pathogens. Proc Natl Acad Sci USA. 2013; 110:3841–3846. [PubMed: 23431180]

DeLano, WL. The PyMOL molecular graphics system. DeLano Scientific; Palo Alto: 2002.

Dell'Angelica EC, Schleicher CH, Santome JA. Primary structure and binding properties of calgranulin C, a novel S100-like calcium-binding protein from pig granulocytes. J Biol Chem. 1994; 269:28929–28936. [PubMed: 7961855]

Donato R. Intracellular and extracellular roles of S100 proteins. Microsc Res Tech. 2003; 60:540–551. [PubMed: 12645002]

Donato R, Cannon BR, Sorci G, Riuzzi F, Hsu K, Weber DJ, Geczy CL. Functions of S100 proteins. Curr Mol Med. 2013; 13:24–57. [PubMed: 22834835]

Fritz G, Heizmann CW, Kroneck PM. Probing the structure of the human Ca^{2+}- and Zn^{2+}-binding protein S100A3: spectroscopic investigations of its transition metal ion complexes, and three-dimensional structural model. Biochim Biophys Acta. 1998; 1448:264–276. [PubMed: 9920417]

Fritz G, Mittl PR, Vasak M, Grutter MG, Heizmann CW. The crystal structure of metal-free human EF-hand protein S100A3 at 1.7-A resolution. J Biol Chem. 2002; 277:33092–33098. [PubMed: 12045193]

Günter, F.; Heizmann, CW. Handbook of Metallproteins. 2006. 3D Structures of the Calcium and Zinc Binding S100 Proteins..

Gaddy JA, Radin JN, Loh JT, Piazuelo MB, Kehl-Fie TE, Delgado AG, Ilca FT, Peek RM, Cover TL, Chazin WJ, Skaar EP, Scott Algood HM. The host protein calprotectin modulates the *Helicobacter pylori* cag type IV secretion system via zinc sequestration. PLoS Pathog. 2014; 10:e1004450. [PubMed: 25330071]

Gagnon DM, Brophy MB, Bowman SE, Stich TA, Drennan CL, Britt RD, Nolan EM. Manganese binding properties of human calprotectin under conditions of high and low calcium: X-ray crystallographic and advanced electron paramagnetic resonance spectroscopic analysis. J Am Chem Soc. 2015; 137:3004–3016. [PubMed: 25597447]

Gribenko AV, Makhatadze GI. Oligomerization and diva-lent ion binding properties of the S100P protein: a Ca^{2+}/Mg^{2+}-switch model. J Mol Biol. 1998; 283:679–694. [PubMed: 9784376]

Haase-Kohn C, Wolf S, Lenk J, Pietzsch J. Copper-mediated cross-linking of S100A4, but not of S100A2, results in proinflammatory effects in melanoma cells. Biochem Biophys Res Commun. 2011; 413:494–498. [PubMed: 21924240]

Haley KP, Delgado AG, Piazuelo MB, Mortensen BL, Correa P, Damo SM, Chazin WJ, Skaar EP, Gaddy JA. The human antimicrobial protein calgranulin C participates in control of *Helicobacter pylori* growth and regulation of virulence. Infect Immun. 2015; 83:2944–2956. [PubMed: 25964473]

Hayden JA, Brophy MB, Cunden LS, Nolan EM. High-affinity manganese coordination by human calprotectin is calcium-dependent and requires the histidine-rich site formed at the dimer interface. J Am Chem Soc. 2013; 135:775–787. [PubMed: 23276281]

Heizmann CW, Cox JA. New perspectives on S100 proteins: a multi-functional Ca^{2+}-, Zn^{2+}- and Cu^{2+}-binding protein family. Biometals. 1998; 11:383–397. [PubMed: 10191501]

Heizmann CW, Fritz G, Schäfer BW. S100 proteins: structure, functions and pathology. Front Biosci. 2002; 7:d1356–1368. [PubMed: 11991838]

Hood MI, Mortensen BL, Moore JL, Zhang Y, Kehl-Fie TE, Sugitani N, Chazin WJ, Caprioli RM, Skaar EP. Identification of an *Acinetobacter baumannii* zinc acquisition system that facilitates resistance to calprotectin-mediated zinc sequestration. PLoS Pathog. 2012; 8:e1003068. [PubMed: 23236280]

Ikura M. Calcium binding and conformational response in EF-hand proteins. Trends Biochem Sci. 1996; 21:14–17. [PubMed: 8848832]

Kehl-Fie TE, Chitayat S, Hood MI, Damo S, Restrepo N, Garcia C, Munro KA, Chazin WJ, Skaar EP. Nutrient metal sequestration by calprotectin inhibits bacterial superoxide defense, enhancing neutrophil killing of *Staphylococcus aureus*. Cell Host Microbe. 2011; 10:158–164. [PubMed: 21843872]

Kehl-Fie TE, Zhang Y, Moore JL, Farrand AJ, Hood MI, Rathi S, Chazin WJ, Caprioli RM, Skaar EP. MntABC and MntH contribute to systemic *Staphylococcus aureus* infection by competing with calprotectin for nutrient manganese. Infect Immun. 2013; 81:3395–3405. [PubMed: 23817615]

Kizawa K, Jinbo Y, Inoue T, Takahara H, Unno M, Heizmann CW, Izumi Y. Human S100A3 tetramerization propagates Ca^{2+}/Zn^{2+} binding states. Biochim Biophys Acta. 2013a; 1833:1712–1719. [PubMed: 22846892]

Kizawa K, Unno M, Takahara H, Heizmann CW. Purification and characterization of the human cysteine-rich S100A3 protein and its pseudo citrullinated forms expressed in insect cells. Methods Mol Biol. 2013b; 963:73–86. [PubMed: 23296605]

Koch M, Bhattacharya S, Kehl T, Gimona M, Vasak M, Chazin W, Heizmann CW, Kroneck PM, Fritz G. Implications on zinc binding to S100A2. Biochim Biophys Acta. 2007; 1773:457–470. [PubMed: 17239974]

Kordowska J, Stafford WF, Wang CL. Ca^{2+} and Zn^{2+} bind to different sites and induce different conformational changes in human calcyclin. Euro J Biochem. 1998; 253:57–66.

Korndorfer IP, Brueckner F, Skerra A. The crystal structure of the human (S100A8/S100A9)2 heterotetramer, calprotectin, illustrates how conformational changes of interacting alpha-helices can determine specific association of two EF-hand proteins. J Mol Biol. 2007; 370:887–898. [PubMed: 17553524]

Leon R, Murray JI, Cragg G, Farnell B, West NR, Pace TC, Watson PH, Bohne C, Boulanger MJ, Hof F. Identification and characterization of binding sites on S100A7, a participant in cancer and inflammation pathways. Biochemistry. 2009; 48:10591–10600. [PubMed: 19810752]

Lin J, Yang Q, Yan Z, Markowitz J, Wilder PT, Carrier F, Weber DJ. Inhibiting S100B restores p53 levels in primary malignant melanoma cancer cells. J Biol Chem. 2004; 279:34071–34077. [PubMed: 15178678]

Linse S, Chazin WJ. Quantitative measurements of the cooperativity in an EF-hand protein with sequential calcium binding. Protein Sci. 1995; 4:1038–1044. [PubMed: 7549868]

Malashkevich VN, Dulyaninova NG, Ramagopal UA, Liriano MA, Varney KM, Knight D, Brenowitz M, Weber DJ, Almo SC, Bresnick AR. Phenothiazines inhibit S100A4 function by inducing protein oligomerization. Proc Natl Acad Sci USA. 2010; 107:8605–8610. [PubMed: 20421509]

Maler L, Sastry M, Chazin WJ. A structural basis for S100 protein specificity derived from comparative analysis of apo and Ca^{2+}-calcyclin. J mol biol. 2002; 317:279–290. [PubMed: 11902843]

Moore BW. A soluble protein characteristic of the nervous system. Biochem Biophys Res Commun. 1965; 19:739–744. [PubMed: 4953930]

Moroz OV, Antson AA, Dodson EJ, Burrell HJ, Grist SJ, Lloyd RM, Maitland NJ, Dodson GG, Wilson KS, Lukanidin E, Bronstein IB. The structure of S100A12 in a hexameric form and its proposed role in receptor signalling. Acta Crystallogr D Biol Crystallogr. 2002; 58:407–413. [PubMed: 11856825]

Moroz OV, Antson AA, Grist SJ, Maitland NJ, Dodson GG, Wilson KS, Lukanidin E, Bronstein IB. Structure of the human S100A12-copper complex: implications for host-parasite de-fence. Acta Crystallogr D Biol Crystallogr. 2003; 59:859–867. [PubMed: 12777802]

Moroz OV, Blagova EV, Wilkinson AJ, Wilson KS, Bronstein IB. The crystal structures of human S100A12 in apo form and in complex with zinc: new insights into S100A12 oligomerisation. J Mol Biol. 2009a; 391:536–551. [PubMed: 19501594]

Moroz OV, Burkitt W, Wittkowski H, He W, Ianoul A, Novitskaya V, Xie J, Polyakova O, Lednev IK, Shekhtman A, Derrick PJ, Bjoerk P, Foell D, Bronstein IB. Both Ca^{2+} and Zn^{2+} are essential for S100A12 protein oligomerization and function. BMC Biochem. 2009b; 10:11. [PubMed: 19386136]

Moroz OV, Burkitt W, Wittkowski H, He W, Ianoul A, Novitskaya V, Xie J, Polyakova O, Lednev IK, Shekhtman A, Derrick PJ, Bjoerk P, Foell D, Bronstein IB. Both Ca^{2+} and Zn^{2+} are essential for s100a12 protein oligomerization and function. BMC Biochem. 2009; 10:11. [PubMed: 19386136]

Moroz OV, Wilson KS, Bronstein IB. The role of zinc in the S100 proteins: insights from the X-ray structures. Amino Acids. 2011; 41:761–772. [PubMed: 20306096]

Murray JI, Tonkin ML, Whiting AL, Peng F, Farnell B, Cullen JT, Hof F, Boulanger MJ. Structural characterization of S100A15 reveals a novel zinc coordination site among S100 proteins and altered surface chemistry with functional implications for receptor binding. BMC Struct Biol. 2012; 12:16. [PubMed: 22747601]

Nakashige TG, Zhang B, Krebs C, Nolan EM. Human calprotectin is an iron-sequestering host-defense protein. Nat Chem Biol. 2015; 11:765–771. [PubMed: 26302479]

Nelson MR, Chazin WJ. Structures of EF-hand Ca^{2+}-binding proteins: diversity in the organization, packing and response to Ca^{2+} binding. Biometals. 1998; 11:297–318. [PubMed: 10191495]

Nelson MR, Thulin E, Fagan PA, Forsen S, Chazin WJ. The EF-hand domain: a globally cooperative structural unit. Protein Sci. 2002; 11:198–205. [PubMed: 11790829]

Nishikawa T, Lee IS, Shiraishi N, Ishikawa T, Ohta Y, Nishikimi M. Identification of S100b protein as copper-binding protein and its suppression of copper-induced cell damage. J Biol Chem. 1997; 272:23037–23041. [PubMed: 9287301]

Ostendorp T, Diez J, Heizmann CW, Fritz G. The crystal structures of human S100B in the zinc- and calcium-loaded state at three pH values reveal zinc ligand swapping. Biochim Biophys Acta. 2011; 1813:1083–1091. [PubMed: 20950652]

Ostendorp T, Leclerc E, Galichet A, Koch M, Demling N, Weigle B, Heizmann CW, Kroneck PM, Fritz G. Structural and functional insights into RAGE activation by multimeric S100B. EMBO J. 2007; 26:3868–3878. [PubMed: 17660747]

Pei J, Kim BH, Grishin NV. PROMALS3D: a tool for multiple protein sequence and structure alignments. Nucleic Acids Res. 2008; 36:2295–2300. [PubMed: 18287115]

Potts BC, Carlstrom G, Okazaki K, Hidaka H, Chazin WJ. 1H NMR assignments of apo calcyclin and comparative structural analysis with calbindin D9k and S100 beta. Protein Sci. 1996; 5:2162–2174. [PubMed: 8931135]

Potts BC, Smith J, Akke M, Macke TJ, Okazaki K, Hidaka H, Case DA, Chazin WJ. The structure of calcyclin reveals a novel homodimeric fold for S100 Ca^{2+}-binding proteins. Nat Struct Biol. 1995; 2:790–796. [PubMed: 7552751]

Rustandi RR, Baldisseri DM, Drohat AC, Weber DJ. The Ca^{2+}-dependent interaction of s100b(beta beta) with a peptide derived from p53. Biochemistry. 1998; 37:1951–1960. [PubMed: 9485322]

Schäfer BW, Heizmann CW. The S100 family of EF-hand calcium-binding proteins: functions and pathology. Trends Biochem Sci. 1996; 21:134–140. [PubMed: 8701470]

Schäfer BW, Fritschy JM, Murmann P, Troxler H, Durussel I, Heizmann CW, Cox JA. Brain S100A5 is a novel calcium-, zinc-, and copper ion-binding protein of the EF-hand superfamily. J Biol Chem. 2000; 275:30623–30630. [PubMed: 10882717]

Schaub MC, Heizmann CW. Calcium, troponin, calmodulin, S100 proteins: from myocardial basics to new therapeutic strategies. Biochem Biophys Res Commun. 2008; 369:247–264. [PubMed: 17964289]

Sigel, A.; Sigel, H. Manganese and its role in biological processes. Marcel Dekker; New York: 2000.

Sivaraja V, Kumar TK, Rajalingam D, Graziani I, Prudovsky I, Yu C. Copper binding affinity of S100A13, a key component of the FGF-1 nonclassical copper-dependent release complex. Biophys J. 2006; 91:1832–1843. [PubMed: 16766622]

Striz I, Trebichavsky I. Calprotectin-a pleiotropic molecule in acute and chronic inflammation. Physiol Res. 2004; 53:245–253. [PubMed: 15209531]

Sturchler E, Cox JA, Durussel I, Weibel M, Heizmann CW. S100A16, a novel calcium-binding protein of the EF-hand superfamily. J Biol Chem. 2006; 281:38905–38917. [PubMed: 17030513]

Unno M, Kawasaki T, Takahara H, Heizmann CW, Kizawa K. Refined crystal structures of human Ca^{2+}/Zn^{2+}-binding S100A3 protein characterized by two disulfide bridges. J Mol Biol. 2011; 408:477–490. [PubMed: 21377473]

van Dieck J, Teufel DP, Jaulent AM, Fernandez-Fernandez MR, Rutherford TJ, Wyslouch-Cieszynska A, Fersht AR. Posttranslational modifications affect the interaction of S100 proteins with tumor suppressor p53. J Mol Biol. 2009; 394:922–930. [PubMed: 19819244]

Vogl T, Leukert N, Barczyk K, Strupat K, Roth J. Biophysical characterization of S100A8 and S100A9 in the absence and presence of bivalent cations. Biochim Biophys Acta. 2006; 1763:1298–1306. [PubMed: 17050004]

Vorum H, Madsen P, Rasmussen HH, Etzerodt M, Svendsen I, Celis JE, Honoré B. Expression and divalent cation binding properties of the novel chemotactic inflammatory protein psoriasin. Electrophoresis. 1996; 17:1787–1796. [PubMed: 8982613]

Wilder PT, Baldisseri DM, Udan R, Vallely KM, Weber DJ. Location of the Zn^{2+}-binding site on S100B as determined by NMR spectroscopy and site-directed mutagenesis. Biochemistry. 2003; 42:13410–13421. [PubMed: 14621986]

Wilder PT, Varney KM, Weiss MB, Gitti RK, Weber DJ. Solution structure of zinc- and calcium-bound rat S100B as determined by nuclear magnetic resonance spectroscopy. Biochemistry. 2005; 44:5690–5702. [PubMed: 15823027]

Wolf R, Howard OM, Dong HF, Voscopoulos C, Boeshans K, Winston J, Divi R, Gunsior M, Goldsmith P, Ahvazi B, Chavakis T, Oppenheim JJ, Yuspa SH. Chemotactic activity of S100A7 (Psoriasin) is mediated by the receptor for advanced glycation end products and potentiates

inflammation with highly homologous but functionally distinct S100A15. J Immunol. 2008; 181:1499–1506. [PubMed: 18606705]

Zackular JP, Chazin WJ, Skaar EP. Nutritional immunity: S100 proteins at the host-pathogen interface. J Biol Chem. 2015; 290:18991–18998. [PubMed: 26055713]

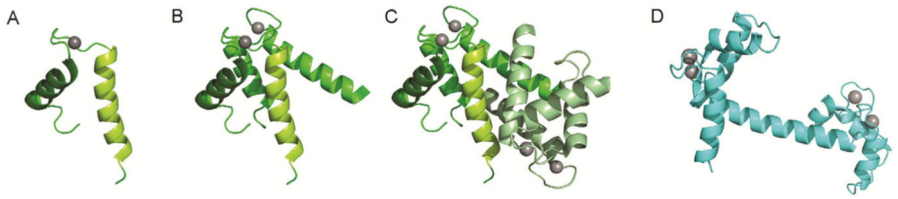

Figure 1.

Structural features of S100 proteins. Ribbon diagrams of (A) an EF-hand motif, (B) an EF-hand domain, (C) the integration of two EF-hand domains into an S100 dimer, and (D) the alternate arrangement of two EF-hand domains in a prototypical EF-hand Ca^{2+} signal modulator. S100A12 was selected as the representative member of the S100 proteins and panels A, B and C were created using the Ca^{2+}-loaded protein (PDB entry 1E8A). Panel D was created using Ca^{2+}-loaded calmodulin (PDB entry 1CLL). The compact nature of the S100 homodimer relative to calmodulin implies a fundamentally different structural mechanism for transduction of Ca^{2+} signals.

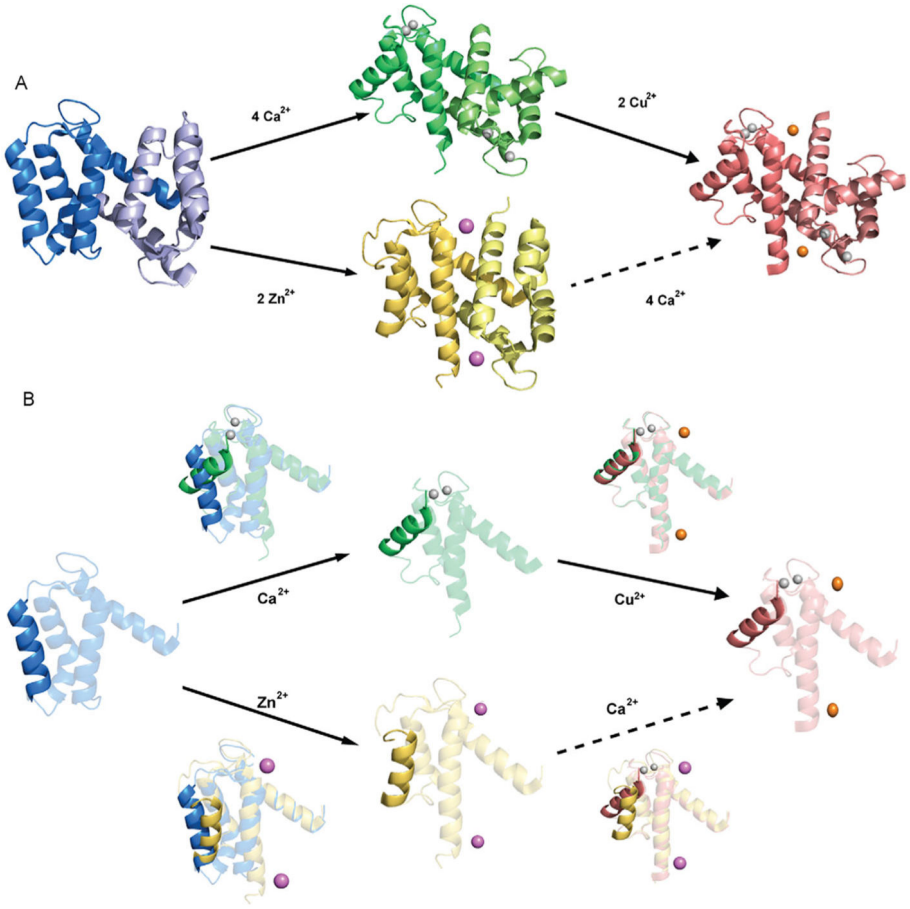

Figure 2.

Three-dimensional structure of S100A12 and conformational changes induced by Ca^{2+} and transition metals. A, Ribbon diagrams of the apo, $(Ca^{2+})_4$, $(Zn^{2+})_2$, and $(Ca^{2+})_4$, $(Cu^{2+})_2$, states. B, Comparison of single sub-units to emphasize the differences in the packing of Helix III in different states. This reveals that the consequences of binding Ca^{2+} are much greater than those of binding transition metals. Images generated in pymol (DeLano, 2002) using coordinates deposited in the PDB for apo (2WCF), $(Ca^{2+})_4$ (1E8A), $(Zn^{2+})_2$ (2WC8) and $(Ca^{2+})_4$, $(Cu^{2+})_2$ (1ODB).

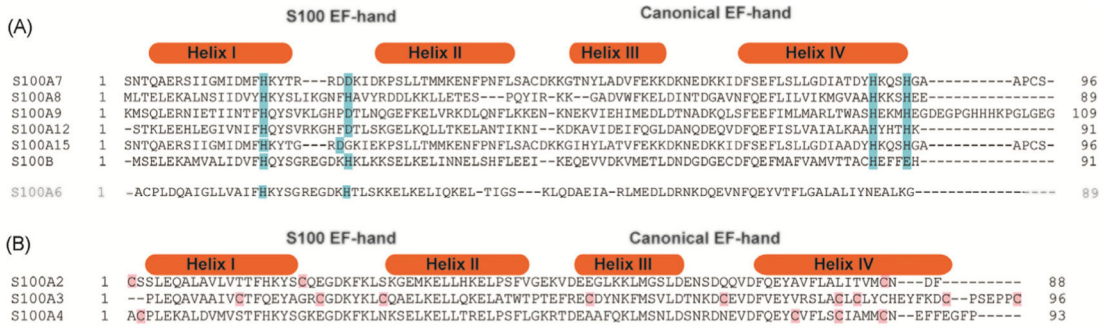

Figure 3.

Alignments of S100 proteins containing transition metal binding sites. Structure based sequence alignment of S100 proteins from the His-rich (upper panel) and Cys-rich (lower panel) categories. Conserved residues in His-rich sites are highlighted with teal background, and those in Cys-rich sites in red background. Note the high degree of conservation in the His-rich proteins compared to the Cys-rich proteins. The alignments were generated using PROMALS3D (Pei et al., 2008).

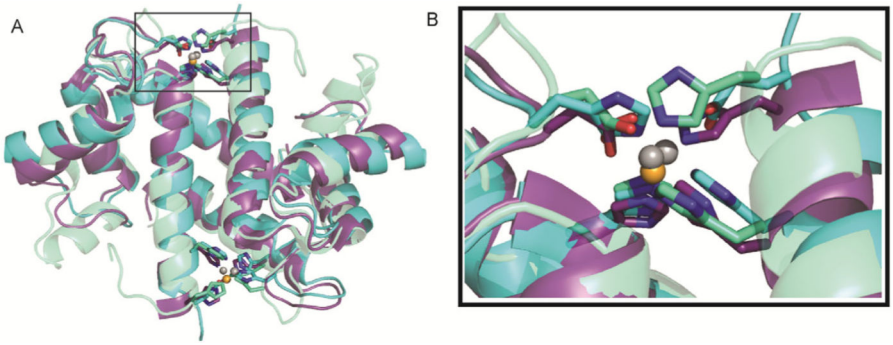

Figure 4.

Structural similarity of tetrahedral zinc and copper binding sites in S100 proteins. A, Overlay of the structures of $(Ca^{2+})_4$, $(Zn^{2+})_2$-S100A7 (light green), $(Ca^{2+})_4$, $(Zn^{2+})_2$-S100B (teal) and $(Ca^{2+})_4$,$(Cu^{2+})_2$-S100A12 (purple) showing that the transition metal ions are chelated in a similar manner by side chains in the same position in the sequence. B, Zoom in on the tetrahedral Zn^{2+} and Cu^{2+} sites showing the similar spatial disposition of the 3 His and 1 Asp chelating side chains. The Zn^{2+} and Cu^{2+} ions are colored gray and orange, respectively. Images generated in pymol (DeLano, 2002) using PDB coordinates deposited for $(Ca^{2+})_4$, $(Zn^{2+})_2$-S100A7 (2PSR), $(Ca^{2+})_4$, $(Zn^{2+})_2$-S100B (3D0Y), and $(Ca^{2+})_4$, $(Cu^{2+})_2$-S100A12 (1ODB).

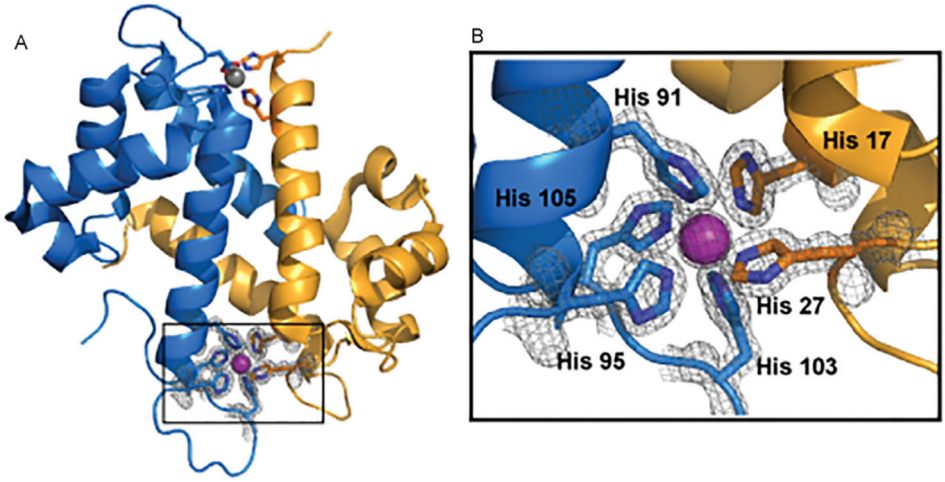

Figure 5.

Three-dimensional structure of calprotectin highlighting the unique manganese binding site. The S100A8 subunit is colored blue, the S100A9 subunit gold, and the Mn^{2+} ion purple. An additional low occupancy Mn^{2+} ion is shown in gray. Images generated in pymol (DeLano, 2002) using coordinates deposited in the PDB for $(Ca^{2+})_4$, (Mn^{2+})-CP (4GGF).

Table 1

S100 protein transition metal binding affinities

Protein	Zn^{2+} K_d	Mn^{2+} K_d	Cu^{2+} K_d
S100A1	$<K_d$ (S100B)		
	Trp fluorescence (Baudier, et al., 1986)		
S100A2	49 nmol L^{-1} (−Ca)		
	25 nmol L^{-1} (+Ca)		
	Competition with Zn chelator (Koch et al., 2007)		
S100A3	4 nmol L^{-1} (−Ca)		
	Competition with Zn chelator (Fritz, et al., 2002)		
S100A5	1–3 μmol L^{-1} (−Ca)		5 μmol L^{-1} (−Ca)
	Equilibrium gel filtration (Schäfer, et al., 2000)		Equilibrium gel filtration (Schäfer et al., 2000)
S100A6	100 nmol L^{-1} (+Ca)		
	Fluorescence spectroscopy (Kordowska, et al., 1988)		
S100A7	100 μmol L^{-1} (−Ca)		
	Equilibrium dialysis (Vorum, et al., 1996)		
S100A8/A9	3 nmol L^{-1} (+Ca) Site1 (Mn/Zn)	6 nmol L^{-1} (+Ca) Site1 (Mn/Zn)	
	8 nmol L^{-1} (+Ca) Site2 (Zn only)	ITC (Damo, et al., 2013)	
	ITC (isothermal titration calorimetry) (Damo, et al., 2013)		
	$K_{d1} \leq 10$ pmol L^{-1} (excess Ca)	K_{d1}=200 nmol L^{-1} (excess Ca)	
	$K_{d2} \leq 240$ pmol L^{-1} (excess Ca)	K_{d2}=20 μmol L^{-1} (excess Ca)	
	Fluorescent competition (Brophy, et al., 2012)	EPR titrations (Hayden et al., 2013)	
S100A12	2 and 100 μmol L^{-1} (−Ca)		
	Fluorescence spectroscopy (Moroz, et al., 2009)		
S100A13			12 and 55 μmol L^{-1} (−Ca)
			62 and 120 μmol L^{-1} (+Ca)
			ITC (Sivaraja, et al., 2006)
S100A16	~ 25 μmol L^{-1} (−Ca)		
	Equilibrium gel filtration (Sturchler et al., 2006)		
S100B	94 nmol L^{-1} (+Ca)	71 μmol L^{-1} (−Ca)	Average 0.46 μmol L^{-1} (−Ca)
	ITC (Wilder et al., 2003)	55.9 μmol L^{-1} (+Ca)	Equilibrium filtration (Nishikawa et al., 1997)
		EPR and NMR (Rustandi et al., 1988)	